Growth and fluorination of CaSi$_2$ thin film

Kenji Ito[1*], Tetsu Ohsuna[1], Takashi Suemasu[2], and Hideyuki Nakano[1]

[1]*TOYOTA CENTRAL R&D LABS., Inc., Nagakute, Aichi 480-1192, Japan*

[2]*Institute of Applied Physics, University of Tsukuba, Tsukuba, Ibaraki 305-8573, Japan*

E-mail: ken-itoh@mosk.tytlabs.co.jp

We fabricated bilayer silicene (BLSi) from an epitaxial CaSi$_2$ thin film grown on a Si (111) substrate followed by treatment with BF$^-_4$-based ionic liquid. First, a 6R-CaSi$_2$ thin film was grown from simultaneously supplied Ca and Si sources. After reacting the CaSi$_2$ thin film with BF$^-_4$-based ionic liquid, the BLSi was formed. The reaction proceeded laterally along the CaSi$_2$ layer. The rearrangement of the Si and Ca atomic layers in the CaSi$_2$ thin film was investigated by high-angle annular dark-field scanning transmission electron microscope images.

1. Introduction

Silicene, a two-dimensional (2D) silicon material with a honeycomb network like graphene, is an attractive candidate in future nano-electronic devices. The 2D structure of monolayer silicene is expected to confer various unique characteristics, such as tunable band gaps[1], a quantum spin Hall effect[2], high-temperature superconductivity[3], and giant magnetoresistance[4]. However, despite recent progress in the epitaxial synthesis of silicene and investigation of its electronic properties[5-13], poor air stability has prevented its application in devices[14]. By reacting $CaSi_2$ and BF_4^--based ionic liquid, Yaokawa et al.[15] recently fabricated a 2D linked silicon network of bilayer silicene (BLSi) sandwiched between CaF_2 crystals. They predicted that BLSi is more stable in air than monolayer silicene because it has a low density of dangling bonds[15]. We therefore focus on $CaSi_2$, an attractive precursor of BLSi. $CaSi_2$ is a distinctive metal silicon compound with a layered structure of buckled Si sheets partitioned by Ca monolayers (Fig. 2(b))[16].

The typical precursors of 2D silicon material are microcrystalline powder and single-crystal platelets of $CaSi_2$[17, 18]. If highly crystalline $CaSi_2$ thin films could be grown on a large-area substrate, we could easily prepare 2D silicon materials with large area. The material properties are much easier to investigate on macro-surfaces than on the small platelets obtained from $CaSi_2$ bulk crystals. Moreover, successful large-scale production is predicted to benefit future device applications.

$CaSi_2$ thin film has been grown on crystalline Si by Ca evaporation. Morar et al.[19, 20] grew thin $CaSi_2$ layers by solid phase epitaxy, whereby the Ca is deposited on Si (111) at room temperature followed by annealing. Vogg et al.[21] deposited Ca on a Si substrate preheated to between 700 and 900 °C. The preheating promoted the reaction of Ca on the substrate surface during reactive deposition epitaxy (RDE), yielding a thick $CaSi_2$ with the same orientation as the substrate. In our previous report[22], we investigated the growth conditions of RDE at low substrate temperature to suppress the Ca desorption from the substrate surface. As the grown silicide films contained both CaSi and $CaSi_2$ phases, we needed to control the RDE condition to obtain single-phase $CaSi_2$. Moreover, $CaSi_2$ has two types of stacking sequences in its trigonal rhombohedral structure, denoted 3R and 6R. We eventually reported that adding a Si source achieved a smooth-surfaced 6R-$CaSi_2$ layer on the Si substrate. The homogenously grown film suppressed the variation of the chemical

reaction rate, which was beneficial for fabricating the silicene structure in the following reaction.

In the present study, we fabricate a CaSi$_2$ thin film on a Si(111) substrate and react it with a BF$^-_4$-based ionic liquid. The aim is to fabricate a wavy (w-) BLSi similar to the bulk material.[15]

2. Experimental methods

A CaSi$_2$ thin film was grown on Si (111) substrate as described in a previous report.[22] The substrate was degreased by ultrasonic cleaning using organic solvents, then cleaned by a combined acid-and-alkali cleaning process. Once installed in the growth chamber, the substrate was heated to over 930 ℃ to remove the protective oxide prior to the silicide growth. After the oxide removal, the substrate temperature was lowered to 560 °C for growing the silicide film. The Ca was fed to the heated Si (111) substrate surface from a Knudsen cell, and the Si source was evaporated by electron beam radiation. The Ca cell temperature was raised at 395 °C, and the Ca deposition rate was approximately 0.4 nm/min. The Si deposition rate was controlled by the beam current of the electron beam gun. The deposition rate of each source material was confirmed using a quartz crystal microbalance. The atomic feeding ratio of Ca/Si was set to almost 2. The growth time of the silicide layer was 46 min. The grown silicide layer was coated with a 15 nm-thick cap layer of amorphous Si at room temperature to prevent oxidation of the silicide surface.

After the growth process, surface protection and lateral reaction process was performed as shown schematically in Fig. 1. The grown film was covered by SiO$_2$ deposited by plasma assisted chemical vapor deposition. The SiO$_2$ layer prevented any direct reaction with the ionic liquid. After the deposition, a portion of this oxide was etched by reactive ion etching to open a starting region for the reaction; that is, an exposed surface of CaSi$_2$ in direct contact with the solution. The CaSi$_2$ grown film with an SiO$_2$-protected surface on the Si(111) substrate was immersed into an ionic liquid, [BMIM][BF$_4$](C$_8$H$_{15}$BF$_4$N$_2$:1-buthyl-3-methylimidazolium tetrafluoroborate), and then heated at 175 °C under an Ar flow for 2–10 hours. The reaction between the thin film and ionic liquid was controlled by exploiting the lateral progress of the reaction. During the treatment, the CaSi$_2$ thin film was reconstructed as BLSi. The treated sample surface was

cleaned by acetonitrile.

The crystal structure was determined from X-ray diffraction (XRD) measurements taken by a Rigaku Ultima-IV diffractometer, and the structural changes in the film plane were investigated by microscopic Raman scattering spectroscopy (Jasco NRS-3300). The excitation laser wavelength and spatial resolution were 532 nm and 1 μm, respectively. The microstructures of the silicide or reacted layer were investigated in cross-sectional images obtained by high-angle annular dark-field scanning transmission electron microscopy (HAADF−STEM) using a JEOL JEM-2100F instrument.

3. Results and discussion

The crystal structure of the grown $CaSi_2$ thin film was confirmed by XRD measurements. Figure 2(a) shows the XRD pattern of the film on the Si substrate, grown from the source materials Ca and Si. The peaks at 17.5º, 35.2º, and 53.5º correspond to the (006) (0012) and (0018) reflection angles of 6R-$CaSi_2$, respectively. The peaks of structures such as 3R-$CaSi_2$ or CaSi were not observed, confirming the growth of single-phase 6R-$CaSi_2$. Therefore, we expected a homogeneous reaction between the film and the ionic liquid.

Initially, the $CaSi_2$ thin films were directly reacted with ionic liquids, as in the $CaSi_2$ bulk case.[15] The treatment was performed under the bulk-case conditions (250 ℃ for 1 hour). Panels (a) and (b) of Fig. 3 show the cross-sectional HAADF−STEM images before and after treatment, respectively. After treatment, the layered structure of $CaSi_2$ was collapsed and disordered, and the expected structural transformation to silicene was not obtained. We surmised that an excess reaction had occurred between the ionic liquid and the film surface.

To confirm the reaction temperature between the ionic liquid and the thin film, we examined the reaction dependence on treatment temperature in a thin film without the SiO_2 layer. Figure 4 shows the XRD patterns before and after treatment at 150 and 170 ℃ for 1 hour, respectively. The $CaSi_2$-related peaks disappeared after the 170 ℃ treatment, indicating that the $CaSi_2$ film reacted with the ionic liquid and changed its structure at this temperature. Therefore, we performed the ionic liquid treatment at 175 ℃. We also attempted to control the reaction between the thin film and ionic liquid by the lateral progress of the reaction. An optical microscope image of the surface is shown in Fig. 5 (a).

The light-blue and deep-blue regions indicate the bare and SiO_2−coated film, respectively. Following the process to protect the grown surface, the sample was immersed in BF_4^--based ionic liquid ([BMIM][BF$_4$]) at 175 ℃ for 10 hours. After reacting with the ionic liquid, the boundary between the bare and SiO_2-covered $CaSi_2$ became a deeper blue in the image, indicating a lateral reaction in this region.

Figure 5(b) shows the Raman scattering spectra at different internal distances from the edge of the SiO_2-covered region (indicated by the arrow in Fig. 5(a)). All spectra were measured in the SiO_2-covered region. The peaks at 347 cm^{-1} and 388 cm^{-1} were attributable to 6R-$CaSi_2$ (A_{1g}(Si2), A_{1g}(Si1))[23]. The intensities of these peaks were almost at the background-signal level near the edge of the SiO_2-covered region, but gradually increased toward the inside. At $x = 7$ μm from the edge, the peak intensities were maximized and no longer changed with distance. This indicates that the $CaSi_2$ film fully reacted with the ionic liquid near the edge, and underwent structural changes. In regions far from $x = 7$ μm, the $CaSi_2$ was unreacted with the ionic liquid.

Figure 5(c) shows the dependence of peak intensity on distance from the edge of the SiO_2-covered region after different treatment times in the ionic liquid. The low and high intensity regions represent the reacted and unreacted regions, respectively. The low intensity region spread as the treating time increased, confirming the lateral expansion of the reacted region between the film and the ionic liquid. From Fig. 5(c), the estimated rate of the lateral reaction was approximately 0.9 μm/h. The optical micrographs also clarified the lateral spread of the reaction region from the edge of the region covered by SiO_2 to the inside.

The microstructure of the fluorine diffusion area was observed in the HAAFD−STEM images of the sample cross-section from the edge of the covered region to 17 μm inside the covered region. Panels (b) and (c) of Fig. 6 were taken near the edge and front of the reaction region estimated from the Raman spectra, respectively. The structures were disorganized with no lattice formations. On the other hand, a lattice image was obtained in Fig. 6(d), and some atomic layer exchange was observed in the area containing $CaSi_2$ in the microscopic Raman spectroscopy (Fig. 5(b)). These findings indicate that a small quantity of F$^-$ ions had considerably diffused along the Ca layers toward the inside, enabling slight reconstruction of the $CaSi_2$ structure.

Figure 7 shows the high magnification HAADF−STEM images and the structural schematics near the area shown in Fig. 6(d), These images were observed on the sample that was thinned by a focused ion beam. The bright dots and slanted bars represent the Ca atoms and Si dimers, respectively. The reconstruction of the Ca and Si layers is clearly visible, and the BLSi exhibits inversion (i-) and mirror (m-) symmetry[15]. The formation of such BLSi was predicted by Morishita et al.[24] from molecular-dynamics simulation of Si atoms confined between two parallel-plane walls. BLSi is double-layer Si with hexagonal diamond structure consisting of distorted tetrahedral bonds. Yaokawa et al. also reported the same BLSi in the bulk $CaSi_2$ with low F-concentration treated with [BMIM][BF_4], and discussed a model for the transformation process from a monolayer silicene in $CaSi_2$ to BLSi. The diffusion of F^- ions along the Ca layer is the key to transform the bonding structure under a low temperature by changing the ionic interaction among Si, Ca, and F. We thus confirmed that BLSi was fabricated in the $CaSi_2$ thin film through a lateral reaction process in the region of small fluoride concentration. After suppressing the reaction between the ionic liquid and film surface, the SiO_2-covered surface was an effective surface-protective layer.

However, we could not obtain the wavy (w-) BLSi reported by Yaokawa et al.[15, 25]. They discussed the transformation process from monolayer silicene in single-crystal $CaSi_2$ to w-BLSi. They reported that in the low fluoride-concentration region, the i- and m-BLSi regions shown in Fig. 7 are stabilized with coexisting $CaSi_2$. Stabilization occurs by charge transfer from the Ca atoms that saturate the silicon dangling bonds. With increasing the fluoride concentration, the electrons for Ca−Si bonding was reduced by the diffusion of F^- ion. The changing ionic interactions among the Si, Ca, and F elements destabilize the honeycomb structure of i- or m-BLSi and transform it to w-BLSi. So the formation of i- or m-BLSi is the preliminary step to obtain w-BLSi by reacting it with additional F^- ion. We conclude that the F^- ion supply to $CaSi_2$ in our process was insufficient to form w-BLSi and additional F^- ion is needed to form w-BLSi from $CaSi_2$ thin layer.

4. Conclusions

We fabricated BLSi from $CaSi_2$ thin films grown on a Si substrate followed by treatment in BF_4^--based ionic liquid. Single-phase 6R-$CaSi_2$ was grown on the Si (111) substrate by

simultaneously feeding the Ca and Si sources. A SiO_2 surface layer suppressed the reaction between the silicide and BF_4^--based ionic liquid. HAADF–STEM observations confirmed that in the laterally reacted $CaSi_2$ under the SiO_2 layer, the silicide was reconstructed as i- and m-BLSi. This reconstruction is the preliminary step of transformation to w-BLSi. To meet our ultimate goal (fabricating wafer-scale silicene devices), we believe that w-BLSi can be obtained by optimizing the F concentration in the $CaSi_2$ thin film.

Acknowledgments

Figure Captions

Fig. 1. Schematics of the surface protection and lateral reaction processes.

Fig. 2. (a) XRD pattern of the $CaSi_2$ thin film grown by supplying Ca and Si as source materials, and (b) schematic model of layered lattice structure of 6R-$CaSi_2$.

Fig. 3. Cross-sectional HAADF−STEM images of (a) untreated $CaSi_2$ thin film, and (b) $CaSi_2$ directly treated with [BMIM][BF_4] at 250 °C for 1 hour.

Fig. 4. XRD patterns of the films before and after treatment with [BMIM][BF_4] at 150 and 170 °C.

Fig. 5. (a) Optical micrograph of the SiO_2-covered edge region after the ionic liquid treatment, (b) Raman scattering spectra at different distances x from the edge of the SiO_2-covered region, and (c) peak Raman intensity of 6R-$CaSi_2$ versus distance from the edge after different treatment times in ionic liquid.

Fig. 6. Cross-sectional STEM images at different distances x from the edge of the SiO_2-covered region to the interior: (a) schematic image of sample cross-section, (b) $x =$ 0.5 µm, (c) $x = 8$µm, and (d) $x = 16$µm.

Fig. 7. Fine-structure images of cross-sectional HAADF−STEM. A, C: i-BLSi, B: m-BLSi.[15] red circles: Ca, blue circles; Si.
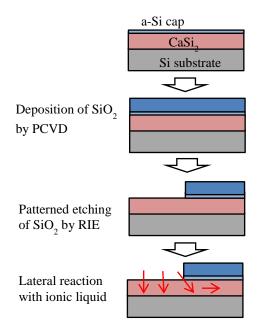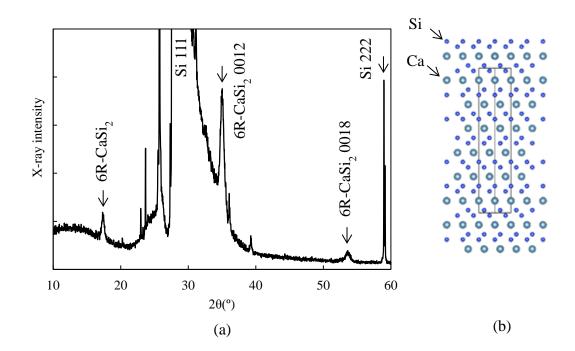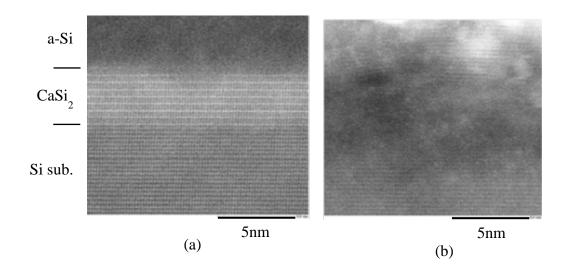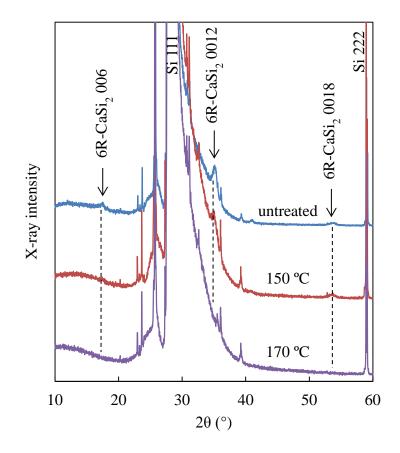
a-Si cap

CaSi$_2$

Si substrate

Deposition of SiO$_2$
by PCVD

Patterned etching
of SiO$_2$ by RIE

Lateral reaction
with ionic liquid

Fig. 1

(a)

(b)

Fig. 2.

a-Si

CaSi$_2$

Si sub.

5nm

(a)

5nm

(b)

Fig. 3

Fig. 4

CaSi$_2$ ←|→ SiO$_2$-covered region

→ x

Lateral reaction region

(a)

2hr

5hr

10hr

175 ℃

Intensity @388cm^{-1}

Distance x (μm)

(c)

Si sub.

6R-CaSi$_2$

175 ℃×10hr

x=45

9

8

7

6

5

3

0μm

Signal intensity

Raman shift (cm^{-1})

(b)

Fig. 5.
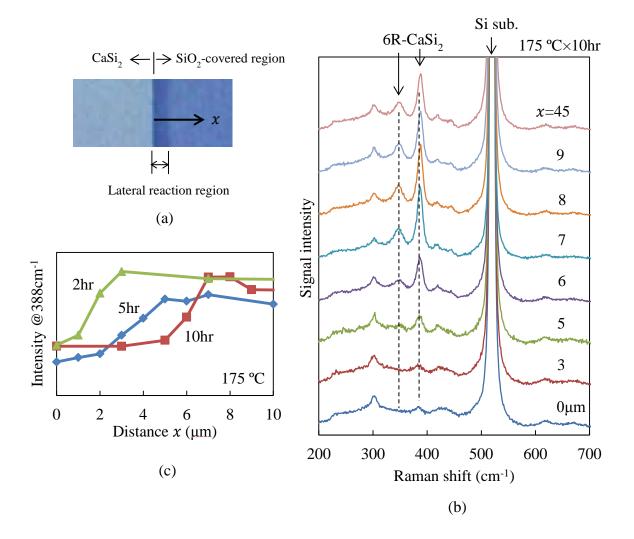
(a)

(b) $x = 0.5$ μm
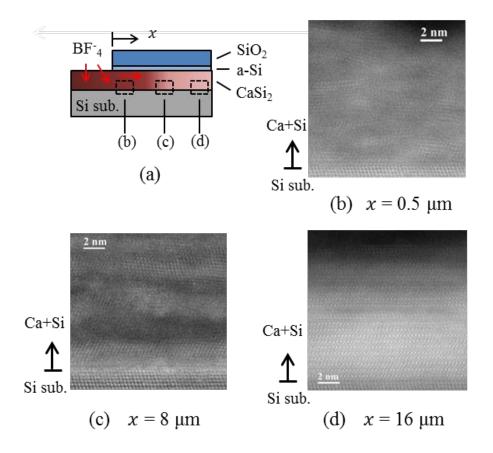
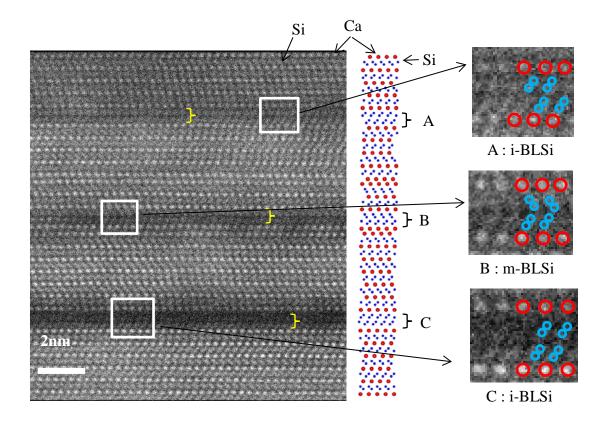(c) $x = 8$ μm

(d) $x = 16$ μm

Fig. 6.

Fig. 7.

References

1) N. D. Drummond, V. Zólyomi, and V. I. Fal'ko, Phys. Rev. B **85**, 075423 (2012).

2) X.-T. An, Y.-Y. Zhang, J.-J. Liu, and S.-S. Li, Appl. Phys. Lett. **102**, 043113 (2013).

3) L. Chen, B. Feng, and K. Wu, Appl. Phys. Lett. **102**, 081602 (2013).

4) S. Rachel and M. Ezawa, Phys. Rev. B **89**, 195303 (2014).

5) C.-L. Lin, R. Arafune, K. Kawahara, N. Tsukahara, E. Minamitani, Y. Kim, N. Takagi and M. Kawai, Appl. Phys. Express **5**, 045802 (2012).

6) B. Lalmi, H. Oughaddon, H. Enriquez, A. Kara, S. Vizzini, B. Ealet, and B. Aufray, Appl. Phys. Lett. **97**, 223109 (2010).

7) L. Meng, Y. Wang, L. Zhang, S. Du, R. Wa, L. Li, Y. Zhang, G. Li, H.Zhou, W. A. Hoter, and H.-J. Gao, Nano Lett. **13**, 685 (2013).

8) Y. Yamada-Takamura and R. Friedlein, Sci. Technol. Adv. Mater. **15**, 064404 (2014).

9) A.Fleurence, T. G. Gill, R. Friedlein, J. T. Sadowski, K. Aoyagi, M. Copel, R. M. Tremp, C. F. Hirjibehedin, and Y. Yamada-Takamura, Appl. Phys. Lett. **108**, 151902 (2016).

10) A. Fleurence, R. Friedlein, T. Ozaki, H. Kawai, Y. Wang, and Y. Yamada-Takamura, Phys. Rev. Lett. **108**, 24550 (2012).

11) T. Aizawa, S. Suehara, and S. Otani, J. Phys.: Condens. Matter. **27**, 305002 (2015).

12) Y. Yamada-Takamura, F. Bussolotti, A. Fleurence, S. Bera, and R. Friedlein, Appl. Phys. Lett. **97**, 073109 (2010).

13) T. Aizawa, S. Suehara, and S.Otani, J. Phys. Chem. C **118**, 23049 (2014).

14) A. Molle, C. Grazianetti, D. Chiappe, E. Cinquanta, E. Cianci, G. Tallarida, and M. Fanciulli, Adv. Funct. Mater. **23**, 4340 (2013).

15) R. Yaokawa, T. Ohsuna, T. Morishita, Y. Hayasaka, M. J. S. Spencer, and H. Nakano, Nat. Commun. **7**, 10657 (2016).

16) O. Bisi, L. Braicovich, C. Carbone, I. I. Lindau, A. Iandelli, G. L. Olcese, and A. Palenzona, Phys. Rev. B **40**, 10194 (1989).

17) U. Dettlaff-Weglikowska, W. Hönle, A. Molassioti-Dohms, S. Finkbeiner, and J. Webe, Phys. Rev. B **56,** 13132 (1997).

18) J. R. Dahm, B. M. Way, E. Fuller, and J. S. Tse, Phys. Rev. B **48**, 17872 (1993).

19) J. F. Morar and M. Wittmer, Phys. Rev. B **37**, 2618 (1988).

20) J. F. Morar and M. Wittmer, J. Vac. Sci. Technol. A **6**, 1340 (1988).

21) G.Vogg, M. S. Brandt, M. Stutzmann, and M. Albrecht, J. Cryst. Growth **203**, 570 (1999).

22) K. Ito, T. Suemasu, and H. Nakano, Jpn. J. Appl. Phys. **57**, 120313 (2018).

23) S. M. Castillo, Z. Tang, A. P. Litvinchuk, and A. M. Guloy, Inorg. Chem. **55**, 10203 (2016).

24) T. Morishita, K. Nishio and M. Mikami, Phys. Rev. B **77**, 081401 (2008).

25) R. Yaokawa, T. Ohsuna, Y. Hayasaka, and H. Nakano, Chemistry Select **1**, 5579 (2016).